



Article

Self-Assembling Systems Based on Pillar[5]arenes and Surfactants for Encapsulation of Diagnostic Dye DAPI

Anastasia Nazarova , Arthur Khannanov, Artur Boldyrev , Luidmila Yakimova * and Ivan Stoikov *

A.M. Butlerov' Chemistry Institute of Kazan Federal University, 18 Kremlyovskaya Str., 420008 Kazan, Russia; anas7tasia@gmail.com (A.N.); arthann@gmail.com (A.K.); boldyrev25@gmail.com (A.B.)

* Correspondence: mila.yakimova@mail.ru (L.Y.); ivan.stoikov@mail.ru (I.S.);
Tel.: +7-843-233-72-41 (L.Y.); +7-843-233-7241 (I.S.)

Abstract: In this paper, we report the development of the novel self-assembling systems based on oppositely charged Pillar[5]arenes and surfactants for encapsulation of diagnostic dye DAPI. For this purpose, the aggregation behavior of synthesized macrocycles and surfactants in the presence of Pillar[5]arenes functionalized by carboxy and ammonium terminal groups was studied. It has been demonstrated that by varying the molar ratio in Pillar[5]arene-surfactant systems, it is possible to obtain various types of supramolecular systems: host-guest complexes at equimolar ratio of Pillar[5]arene-surfactant and interpolyelectrolyte complexes (IPECs) are self-assembled materials formed in aqueous medium by two oppositely charged polyelectrolytes (macrocycle and surfactant micelles). It has been suggested that interaction of Pillar[5]arenes with surfactants is predominantly driven by cooperative electrostatic interactions. Synthesized stoichiometric and non-stoichiometric IPECs specifically interact with DAPI. UV-vis, luminescent spectroscopy and molecular docking data show the structural feature of dye-loaded IPEC and key role of the electrostatic, π - π -stacking, cation- π interactions in their formation. Such a strategy for the design of supramolecular Pillar[5]arene-surfactant systems will lead to a synergistic interaction of the two components and will allow specific interaction with the third component (drug or fluorescent tag), which will certainly be in demand in pharmaceuticals and biomedical diagnostics.

Keywords: Pillar[5]arene; complexation; DAPI; interpolyelectrolyte; self-assembly; surfactant; visualization system; drug delivery system



Citation: Nazarova, A.; Khannanov, A.; Boldyrev, A.; Yakimova, L.; Stoikov, I. Self-Assembling Systems Based on Pillar[5]arenes and Surfactants for Encapsulation of Diagnostic Dye DAPI. *Int. J. Mol. Sci.* **2021**, *22*, 6038. <https://doi.org/10.3390/ijms22116038>

Academic Editors: Lucia Ya. Zakharova and Ruslan R. Kashapov

Received: 19 May 2021
Accepted: 31 May 2021
Published: 3 June 2021

Publisher's Note: MDPI stays neutral with regard to jurisdictional claims in published maps and institutional affiliations.



Copyright: © 2021 by the authors. Licensee MDPI, Basel, Switzerland. This article is an open access article distributed under the terms and conditions of the Creative Commons Attribution (CC BY) license (<https://creativecommons.org/licenses/by/4.0/>).

1. Introduction

The controlled self-assembly of polyfunctional structures into various types of associates opens up wide opportunities for design-targeted drug delivery systems and imaging systems. The implementation of supramolecular chemistry into biomedicine makes it possible to increase the bioavailability, prolong the action of the drug, and prevent its premature degradation, which significantly affects the decrease in the number of side effects and the increase in the therapeutic efficacy of the drug [1–3].

The use of Pillar[5]arenes as a macrocyclic component is especially attractive due to the possibility of modification by various functional groups on both sides of the macrocyclic platform [4,5]. Pillar[5]arenes are capable of forming complexes with various biologically significant substrates using their hydrophobic macrocyclic cavity or substituents on both rims of the macrocycle [6–10]. Directed functionalization of Pillar[5]arenes allows one to control such important properties of molecules as bioavailability and water solubility [11–15]. Effective binding of the substrate can be carried out either due to the hydrophobic cavity or due to functional groups [16–22]. The cooperative action of the cavity and substituents is particularly characteristic during the complexation of charged macrocycles and a substrate, for example, surfactant molecules [23–27]. As a result, 1:1 host-guest complexes are formed [28–35]. In addition, the ability of water-soluble macrocycles, by analogy with non-macrocyclic surfactants, to form various types of associates

such as liposomes [36–38], micelles [39–41], and liquid crystals [42,43], etc., is well known. It attracts great attention due to their potential application in various fields and especially in biomedicine as nanocontainers for medicinal and imaging agents [44–51]. Consequently, it becomes possible to obtain both host–guest complexes and polyelectrolyte aggregates of macrocycle-surfactants by varying the stoichiometric composition of a Pillar[5]arene-surfactant mixture on the analogy of interpolyelectrolyte complexes (IPEC) based on oppositely charged polymers [52–57].

The use of IPEC as drug delivery systems or imaging systems is attracting more and more attention of researchers due to the environmental friendliness and safety of such systems [58,59]. Most of the IPEC can be obtained in aqueous media without the use of organic solvents and chemical crosslinking agents by mixing oppositely charged solutions of polyelectrolytes in different ratios. A promising direction in the design of IPEC is the use of macrocyclic compounds, which, due to the presence of a macrocyclic cavity, make it possible to obtain materials with a specified structure and properties [60–62]. The interaction of the macrocyclic platform with oppositely charged polyelectrolyte molecules leads to a change in the properties of the supramolecular complex due to the cooperative aggregation of its components [39,63]. The polyelectrolyte, the role of which can be played by various surfactants, can change the aggregation and binding properties of the macrocyclic compound. The macrocyclic molecule, in turn, can fix the polyelectrolyte in a predetermined manner in space.

Summarizing the above, it can be argued that such a strategy for the design of interpolyelectrolyte supramolecular Pillar[n]arene-surfactant systems will lead to a synergistic interaction of two components and will allow specific interaction with the third component (drug or fluorescent label), which will certainly be in demand in pharmaceuticals and biomedical diagnostics. Therefore, the aim of this work was to create supramolecular systems based on oppositely charged Pillar[5]arene and surfactants for encapsulating the dye 4',6-diamidino-2-phenylindole (DAPI), which is used for fluorescent staining of DNA in fluorescence microscopy [64,65]. We studied the aggregation behavior of synthesized macrocycles and surfactant molecules and investigated the encapsulating ability of mixed IPECs as nanocontainers for a fluorescent label.

2. Results and Discussion

2.1. Self-Assembly and Characterization of Pillar[5]arene-Surfactant Systems

To obtain stable self-assembling systems based on Pillar[5]arenes and surfactants, the self-assembly of individual components of these systems, namely, macrocycles **1** and **2**, and surfactants sodium dodecyl sulfate (SDS) and dodecyl trimethylammonium chloride (DTAC) was studied. Dynamic light scattering method shows the formation of polydispersity systems with submicron-sized associates for each component at the concentration range 1×10^{-5} to 1×10^{-3} M (Table S1). The main feature of surfactants is their ability to form micelles of various sizes. Pillar[5]arenes are convenient macrocyclic platforms that can form a large number of host–guest complexes with various substrates (surfactants, drugs, etc.). Therefore, various nanosystems were created based on the Pillar[5]arenes (liposomes, micelles, vesicles, nanostructured lipid carriers, etc.). In this regard, we made the assumption that by varying the molar ratio in Pillar[5]arene-surfactant systems, it is possible to create various types of supramolecular systems (Figure 1):

I: host-guest complexes at equimolar ratio of Pillar[5]arene-surfactant.

II: stoichiometric interpolyelectrolyte complexes (SIPEC) are self-assembled materials formed in aqueous media by two oppositely charged polyelectrolytes (macrocycle and surfactant micelles) at equimolar ratio of the charged groups.

III: nonstoichiometric interpolyelectrolyte complexes (NIPEC), where the charges of one sign prevail.

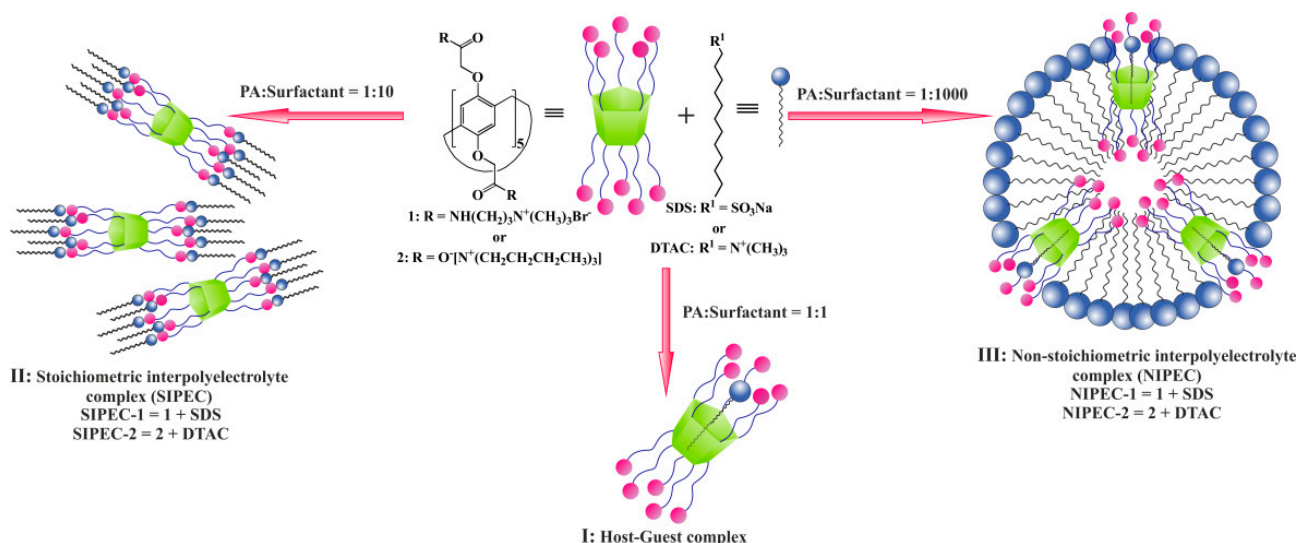


Figure 1. Schematic representation of the formation of different types of aggregates in different ratios of Pillar[5]arene-surfactant.

Tenfold excess of surfactants gives us mixed systems, stoichiometric interpolyelectrolyte complexes (SIPEC), where ten charged groups of Pillar[5]arene electrostatically interact with ten molecules of surfactant. At the same time, the addition of a significant (100- or 1000-fold) excess of surfactant to Pillar[5]arene leads to the formation of surfactant micelles with included Pillar[5]arene molecules, nonstoichiometric interpolyelectrolyte complexes (NIPEC).

2.2. Host–Guest Complexes at Equimolar Ratio of Pillar[5]arene-Surfactant

To describe the formation of various types of systems (I, II, III), we used UV-vis spectroscopy and dynamic light scattering methods. The NMR method, widely used to confirm complexation, is not suitable for these systems, because the complexation process is usually accompanied by the association of macrocycles and surfactants, which leads to broadening of signals in the spectrum and difficulties in their characterization.

At the first stage, the complexing properties of oppositely charged macrocycles and surfactants were studied by UV-vis spectroscopy in water (Figure 2). Solutions of guest-molecules (SDS and DTAC) were added to solutions of compounds 1 and 2 (3×10^{-5} M) in a 1:1 ratio, correspondingly. A deviation of the optical density of the mixture (A_{complex}) from the additive spectrum of components, ($\Sigma A_{\text{mixture}}$), $\Delta A = A_{\text{complex}} - \Sigma A_{\text{mixture}}$, was found, which indicates complexation. In both cases, the complexation was accompanied by a hyperchromic effect and a bathochromic shift at 300 nm.

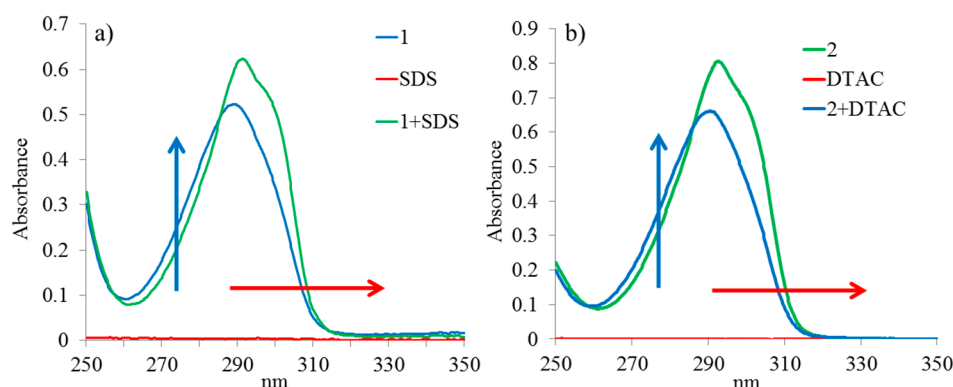


Figure 2. UV-vis absorption spectra: (a) Pillar[5]arene 1/SDS in equimolar ratio in water ($c_{\text{macrocycle}} = 3 \times 10^{-5}$ M, $c_{\text{guest}} = 3 \times 10^{-5}$ M); (b) Pillar[5]arene 2/DTAC at 1:1 ratio in water ($c_{\text{macrocycle}} = 3 \times 10^{-5}$ M, $c_{\text{guest}} = 3 \times 10^{-5}$ M).

To quantify the complexing ability of compounds **1** and **2** with SDS and DTAC, respectively, the association constant K_a and the stoichiometry of the complexes formed were determined. The stoichiometry of the obtained host–guest complexes 1:1 was determined for both complexes by the Job plots (Figure S6). The method of spectrophotometric titration was used to determine the binding constant. For the Pillar[5]arene 1/SDS and Pillar[5]arene 2/DTAC systems, the Pillar[5]arene concentration remained constant, while the surfactant concentration increased from a ratio of 1:0.5 to 1:10 (Figure S3). The data obtained were processed using BindFit [66], and the association constants of the 1:1 complexes were also calculated (Figures S4 and S5). The K_a for 1/SDS was determined as 1053 M^{-1} . The K_a for 2/DTAC was 102 M^{-1} .

2.3. Interpolyelectrolyte Complexes (IPECs) Based on Pillar[5]arene and Surfactant

SIPEC and NIPEC can be formed depending on the molar ratio of cationic to anionic groups. In a stoichiometric complex, positive and negative charges are mutually neutralized, and most of the formed particles can precipitate due to colloidal instability. By contrast, in non-stoichiometric complexes, the forming aggregates contains an excess of one of the polyelectrolytes, thereby conferring the formed particle with surface charge and, in consequence, colloidal stability [67].

So, it was necessary to determine the most optimal molar ratio of Pillar[5]arene to surfactant for formation of SIPEC and NIPEC in water solutions. In this regard, we varied macrocycle:surfactant molar ratio (1:10, 1:100, and 1:1000). For each ratio, the influence of the macrocycle concentration was also investigated ($c_{\text{macrocycle}} = 1 \times 10^{-6} \div 1 \times 10^{-3} \text{ M}$).

To obtain SIPEC, it is necessary to have a minimum 10-fold excess of a surfactant because each of Pillar[5]arenes **1** and **2** have ten charged groups. The amount of surfactant required to obtain SIPEC is also influenced by the basicity and acidity of charged groups and their shielding in self-association processes [68,69]. Indeed, in the case of a 10-fold excess of surfactants in 1/SDS system at a concentration of $1 \times 10^{-3} \text{ M}$ and $1 \times 10^{-4} \text{ M}$, insoluble precipitates are formed. It indicates the **SIPEC-1** formation (Figure 1, I), when positive and negative charges are mutually neutralized, and most of the formed particles precipitate out due to colloidal instability. Therefore, both the aggregate size formed by 1/SDS in the case of a 10-fold excess of surfactants and their dispersity depended weakly on the concentration (Table S2).

The increasing in the SDS content to 1:100 molar ratio at a concentration of 1×10^{-3} and $1 \times 10^{-4} \text{ M}$ results in the fact that precipitates are also formed; however, at a concentration of $1 \times 10^{-5} \text{ M}$, a stable colloidal system with a monomodal size distribution of particles is formed ($d = 242 \pm 9 \text{ nm}$, $\text{PDI} = 0.13$). This behavior of systems is possible with the simultaneous presence of SIPEC and some excess of SDS, which is insufficient to dissolve the precipitate at a relatively high concentration (1×10^{-3} and $1 \times 10^{-4} \text{ M}$). Dilution of the system leads to dissolution of the precipitate and the formation of **NIPEC-1**, with included SDS molecules. This is confirmed by the value of the ζ -potential—the surface of the aggregates is negatively charged ($\zeta = -21 \text{ mV}$). Further dilution ($1 \times 10^{-6} \text{ M}$) leads to destabilization of the system, when the balance of forces of intermolecular interaction and electrostatic repulsion is disturbed, accompanied by coagulation of particles: the particle size and polydispersity of the system increase ($d = 1270 \pm 632 \text{ nm}$, $\text{PDI} = 0.82$).

A further increase in the SDS concentration (1000-fold of SDS) leads to the formation of **NIPEC-1** (Table S2), and at a concentration of $1 \times 10^{-6} \text{ M}$ the most stable particles are formed with a hydrodynamic diameter of $71 \pm 2 \text{ nm}$ and $\text{PDI} = 0.16$. The negative value of the ζ -potential ($\zeta = -40.2 \text{ mV}$) of this system indicates that micelles are formed by surfactant molecules with built-in Pillar[5]arene molecules (Figure 1).

The aggregation behavior of 2/DTAC system is similar to 1/SDS (Table S3), where the formation of IPEC occurs by the same mechanism. At 1:10 stoichiometric ratio, the formation of **SIPEC-2** also occurs. However, no visually insoluble precipitate was found. This is possible due to the predominance of soluble IPECs over insoluble ones, or soluble IPECs are products of incomplete interactions [57,70], due to different strengths of polyelec-

trolytes. In this case, the free units of the initial polyelectrolytes, which did not interact, act as hydrophilic fragments, contributing to the retention of IPEC particles in solution. These assumptions are confirmed by the formation of a stable system with a hydrodynamic particle diameter of 286 ± 13 nm, PDI = 0.23, $\zeta = -34.7$ mV at the concentration of Pillar[5]arene **2** of 1×10^{-4} M. The negative value of the ζ -potential indicates the uncompensation of charges on the surface of micelles, which consist mainly of molecules of macrocycle **2**. In the case of a 1000-fold excess of DTAC with respect to Pillar[5]arene **2**, NIPEC-2 are also formed ($d = 170 \pm 8$ nm, PDI = 0.27, $\zeta = -21$ mV).

Thus, by varying the molar ratio of macrocycle: surfactant, three types of systems were obtained: host-guest complexes at equimolar ratio of Pillar[5]arene-surfactant, SIPEC and NIPEC at surfactant excess.

2.4. DAPI Association with IPEC

Synthesized SIPEC and NIPEC due to non-covalent interactions are capable of specific interaction with a third component represented by a fluorescent label (imaging system agent) or a drug (drug delivery system). 4',6-Diamidino-2-phenylindole (DAPI) is a widespread fluorescent dye that has an affinity for DNA. In addition, DAPI can be used as an antiparasitic, antibiotic, antiviral and antitumor agent. In this regard, we chose DAPI as a guest (third component) to study the interaction with interpolyelectrolyte systems formed by Pillar[5]arene and surfactant molecules. We used UV-vis, fluorescence spectroscopy, nanoparticle trajectory analysis, and dynamic light scattering (DLS) methods for detecting the interaction between the IPEC (SIPEC and NIPEC) and DAPI. Pillar[5]arenes and dye were taken in equimolar ratios ($c = 3 \times 10^{-5}$ M). To assess the possible advantages of using macrocycle/surfactant IPEC for DAPI encapsulation, we additionally investigated the interaction of DAPI with each of the IPEC components, in those concentrations and ratios of the starting components that were used to create the IPEC.

2.4.1. UV-Vis Spectroscopy

UV spectrum of **1**/DAPI mixture shows that macrocycle **1**, containing ten ammonium fragments, does not interact with DAPI (Figure S7). The addition of a 100-fold excess of SDS to DAPI results in a hypochromic effect and a bathochromic shift in comparison to the additivity of two spectra of the binary system (Figure 3a). The 1000-fold excess of SDS to DAPI results in only bathochromic shift from 340 to 360 nm (Figure 3c). The addition of DAPI to the SIPEC-1 (Figure 3b) and NIPEC-1 (Figure 3d) is accompanied by a bathochromic shift and, additionally for SIPEC-1, an increase in absorption of the mixed solution which indicates the formation of large mixed aggregates that are able to scatter light.

There are no changes in the UV spectrum of the DTAC and DAPI mixture (Figure 4b). The addition of DAPI to Pillar[5]arene **2** is accompanied by a hypochromic effect and a bathochromic shift (Figure 4a). The addition of DAPI to SIPEC-2 also shows a bathochromic shift and a hypochromic effect (Figure 4c). At the same time, for NIPEC-2, no visible changes were observed with the addition of the dye (Figure 4d). In the ternary systems described, three types of interactions can be observed: macrocycle-surfactant, macrocycle-dye, and surfactant-dye. Since the surfactant in both studied concentrations does not interact with the dye molecule, and the addition of macrocycle **2** to DAPI leads to a hypochromic effect and a bathochromic shift, it can be assumed that competitive complexation occurs during the formation of ternary systems. For SIPEC-2, the decisive factor is the interaction between the macrocycle and the dye, which is probably due to the higher value of the association constant for the **2**/DAPI system than the K_a **2**/DTAC. At the same time, for NIPEC-2, a 1000-fold excess of surfactant leads to the destruction of the **2**/DAPI complex and the release of the dye, which does not interact with surfactant molecules due to electrostatic repulsion. Thus, the analysis of the experimental data showed that the formation of ternary systems occurs, first, due to the electrostatic forces arising between the surfactant and dye molecules.

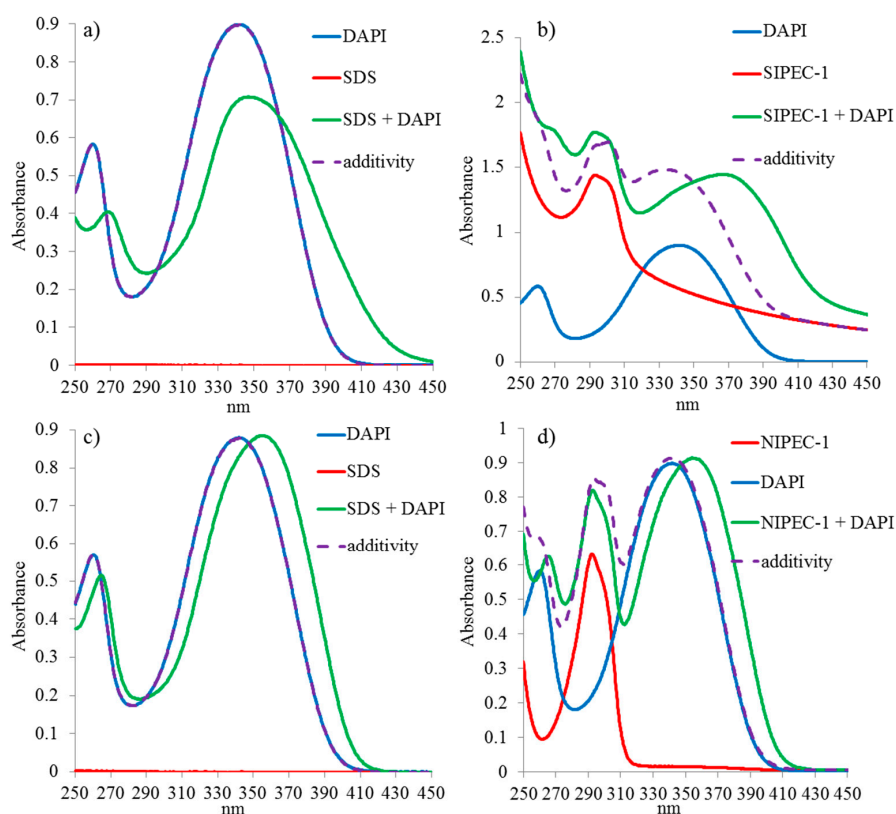


Figure 3. UV-vis absorption spectra: (a) SDS ($c = 3 \times 10^{-3}$ M) + DAPI (3×10^{-5} M); (b) SIPEC-1 + DAPI ($c = 3 \times 10^{-5}$ M); (c) SDS ($c = 3 \times 10^{-2}$ M) + DAPI ($c = 3 \times 10^{-5}$ M); (d) NIPEC-1 + DAPI ($c = 3 \times 10^{-5}$ M).

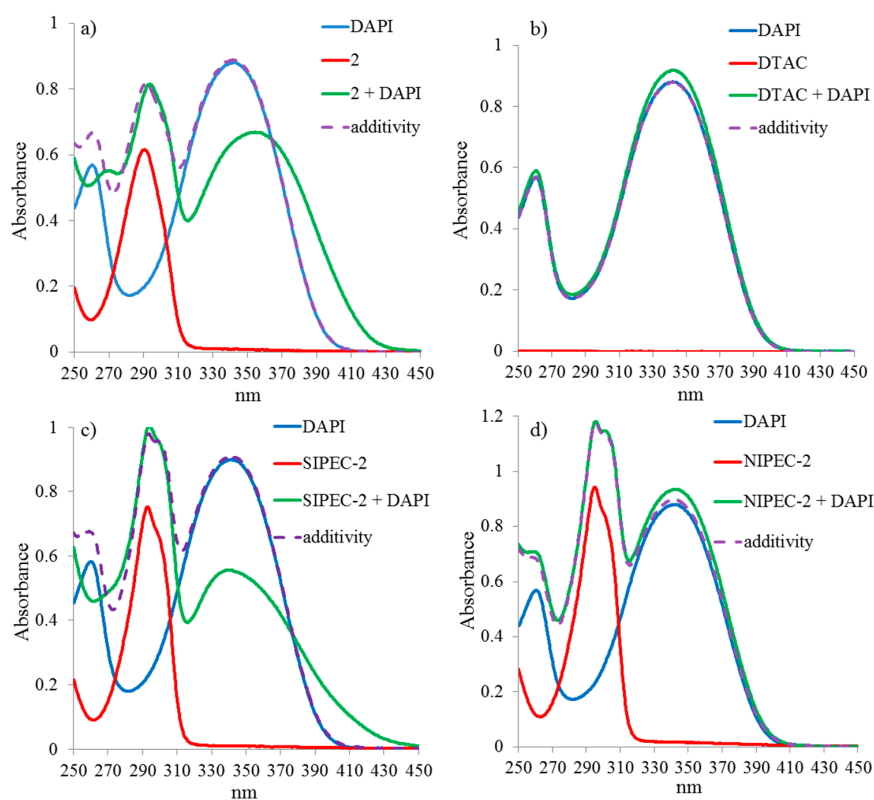


Figure 4. UV-vis absorption spectra: (a) Pillar[5]arene 2 ($c = 3 \times 10^{-5}$ M) + DAPI ($c = 3 \times 10^{-5}$ M); (b) DTAC ($c = 3 \times 10^{-4}$ M) + DAPI ($c = 3 \times 10^{-5}$ M); (c) SIPEC-2 + DAPI ($c = 3 \times 10^{-5}$ M); (d) NIPEC-2 + DAPI ($c = 3 \times 10^{-5}$ M).

2.4.2. Dynamic Light Scattering Method (DLS)

DLS data showed different behavior of interpolyelectrolyte complexes (IPEC-1 and IPEC-2) formed by macrocycles **1** and **2** with respect to DAPI (Table S4). The addition of a dye to **NIPEC-1** only slightly decreased the polydispersity and the size of the ternary system **NIPEC-1**/DAPI aggregates ($d = 215 \pm 28$ nm, PDI = 0.55). A similar behavior is observed for **SIPEC-1**/DAPI: aggregates with a hydrodynamic diameter of 216 ± 2 nm and PDI = 0.06 are formed (Figure S8). DLS data are a good correlate with UV data, where a baseline increase indicated the formation of aggregates (Figure 3b). Thus, the addition of DAPI to **SIPEC-1** ($d = 242 \pm 9$ nm, PDI = 0.13) also slightly decreases the size and PDI of the aggregates formed. According to ζ -potential, the addition of DAPI to **SIPEC-1** (-21 mV) increases the stability of **SIPEC-1**/DAPI aggregates (-36 mV).

For **SIPEC-2**, an opposite behavior is observed: the addition of the dye leads to the enlargement of aggregates and the formation of a system with a wide size range ($d = 494 \pm 133$ nm and PDI = 0.73). At the same time, when DAPI is added to **NIPEC-2**, PDI does not change (PDI = 0.27), and the size of the formed aggregates increases to 683 ± 47 nm (Figure S8). It indicates the aggregation under the action of DAPI. In this case, DAPI molecules stick together **NIPEC-2** aggregates in a certain ordered manner, which only leads to aggregates enlargement without changing the PDI of the system.

2.4.3. Luminescent Spectroscopy, Nanoparticle Trajectory Analysis (NTA) and Molecular Docking

To explain this difference in behavior during the assembly of IPEC with DAPI, we used luminescent spectroscopy and NTA.

Under the experimental conditions similar to UV-vis for Pillar[5]arene **1**, it was shown that the addition of a dye to the macrocycle in the luminescence spectrum of the mixture does not lead to any visible changes (Figure 5a). It is in agreement with the data obtained by UV spectroscopy (Figure S7). The addition of 100-fold excess of SDS to DAPI leads to luminescence flare-up and bathochromic shift (Figure 5b), while with a 1000-fold excess of SDS, only luminescence flare-up occurs (Figure S9a). The similar behavior is observed also for the **NIPEC-1**/DAPI system (Figure S9b). Oppositely, for **SIPEC-1**/DAPI, system luminescence is quenched (Figure 5c). The enhancement of luminescence is due to the electrostatic interaction of acetamidine fragments in the DAPI with a negatively charged aggregate surface (**NIPEC-1** and SDS micelles). Luminescence quenching is apparently due to the shielding of the dye molecule due to incorporation into the **SIPEC-1** structure due to the π - π stacking of the aromatic rings of the Pillar[5]arene **1** and DAPI (Figure 6). The same type of associates is formed in the **SIPEC-2**/DAPI system, where quenching is observed in the luminescence spectra (Figure 6 and Figure S10a).

An unexpected increase in luminescence was observed when a 1000-fold excess of DTAC interacted with DAPI (Figure S10c), while a 100-fold excess of DTAC did not cause any changes in the luminescence spectra (Figure S10b). Obviously, in these systems, DTAC molecules are in different forms (Figure 6). At a high concentration of DTAC (1000-fold excess), DAPI interacts with DTAC micelles, whereas at a lower concentration (100-fold excess), the surfactant molecules are free and the only one electrostatic type of interaction is impossible in this case (Figure 2). In the case of DTAC micelles, a positively charged micelle due to cation- π interactions concentrates dye molecules on the micelle surface, enhancing luminescence (Figure 6 and Figure S10c). By a similar mechanism, DAPI interacts with **NIPEC-2** to induce increased luminescence (Figure 6 and Figure S10d).

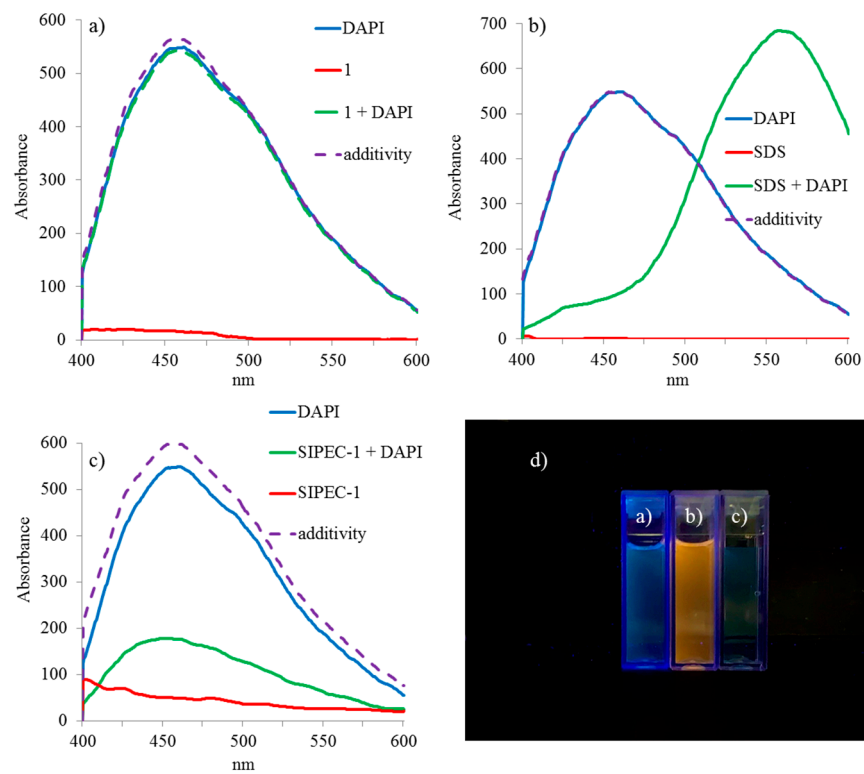


Figure 5. Luminescence spectra: (a) Pillar[5]arene **1** ($c = 3 \times 10^{-5}$ M) + DAPI ($c = 3 \times 10^{-5}$ M); (b) SDS ($c = 3 \times 10^{-3}$ M) + DAPI ($c = 3 \times 10^{-5}$ M); (c) SIPEC-1 + DAPI ($c = 3 \times 10^{-5}$ M); (d) images of solutions a), b), c).

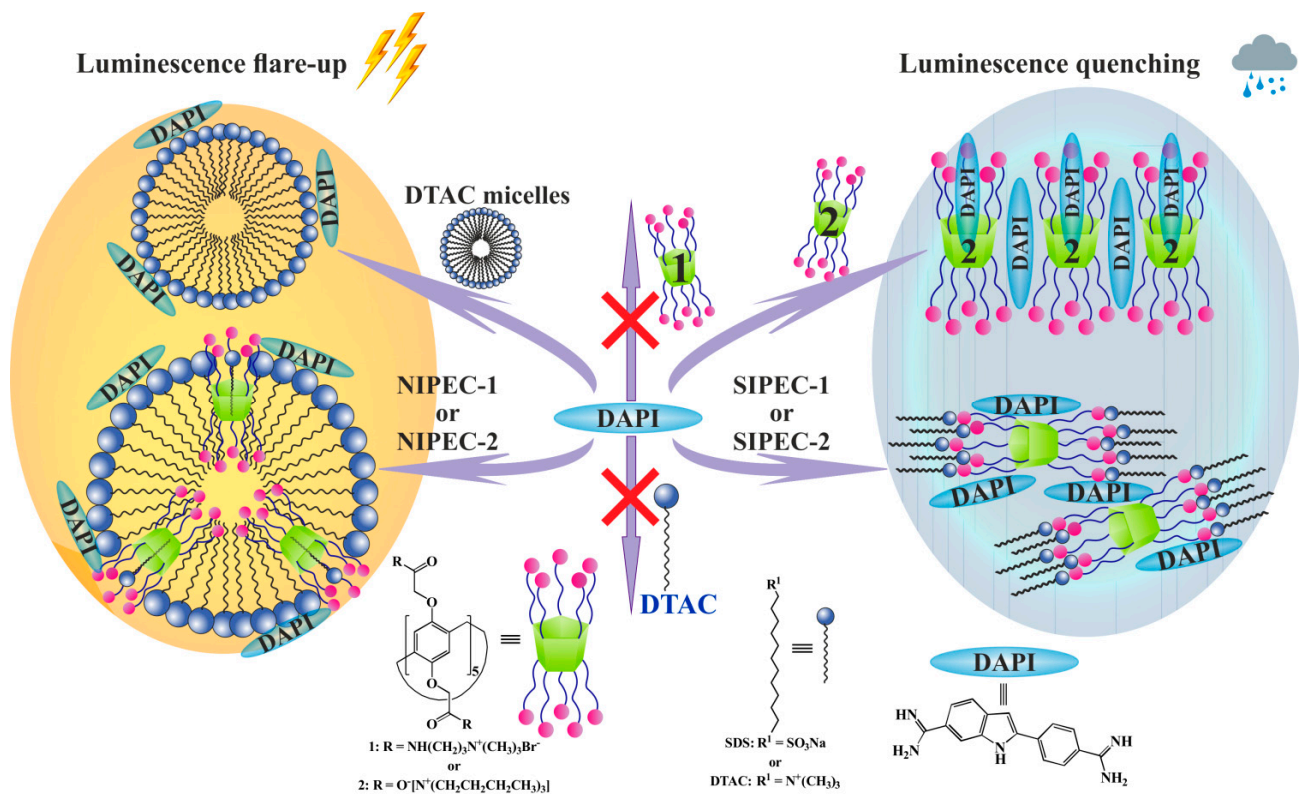


Figure 6. Schematic representation of DAPI interaction with macrocycles **1** and **2**, surfactants, IPEC based on macrocycles and surfactants.

DINC 2.0 web server [71] was used to confirm the fact that luminescence quenching is associated with the inclusion of a dye into the macrocycle cavity and in the structure of associates **SIPEC-1** and **SIPEC-2** due to the π - π stacking of the aromatic rings of the Pillar[5]arene and DAPI (Figure 7). DINC is a parallelized meta-docking method for the incremental docking of ligands. The strategy of DINC involves incrementally docking overlapping fragments with a growing number of atoms, while maintaining the number of flexible bonds constant during this incremental process [72]. The grid size was set to $\sim 30 \text{ \AA} \times 30 \text{ \AA} \times 30 \text{ \AA}$ xyz points and grid center was designated at dimensions (x, y, and z): 0.8, 0.8 and -6.4 .

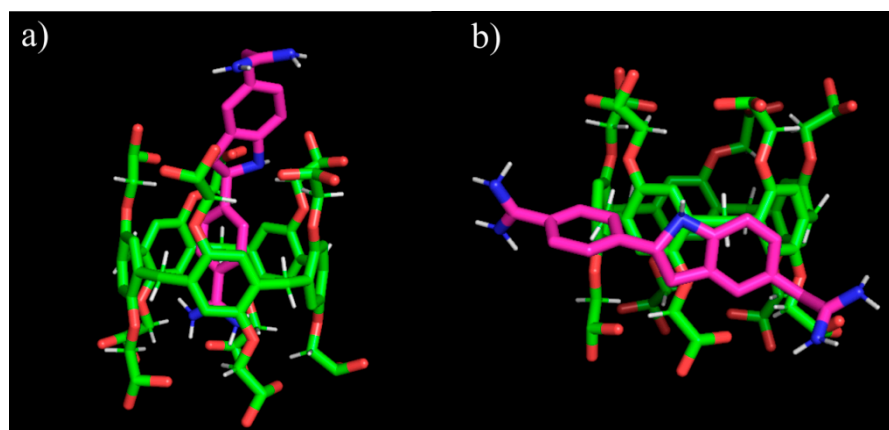


Figure 7. View of the geometry optimized complex formed by macrocycle **2** and 4',6-diamidino-2-phenylindole (DAPI) calculated by DINC 2.0 web server: (a) the dye is inside the cavity; (b) the dye is outside the cavity.

Binding energy in the DINC 2.0 server output between Pillar[5]arene **2** and DAPI (host-guest complex) was -6.30 kcal/mol. The obtained docking results exhibited relatively high potential for binding of DAPI with macrocycle **2** (Figure 7a). This indicates that complexation between the compound **2** and DAPI is an energy efficient process. The location of the dye outside the macrocyclic platform turned out to be energetically favorable (-4.1 kcal/mol). This confirms our assumptions about the structure of **SIPEC**, when the dye molecule is located between macrocycle-surfactant associates (Figure 7b).

Unfortunately, in cases where luminescence increases (SDS/DAPI, DTAC/DAPI, **NIPEC-1**/DAPI, **NIPEC-2**/DAPI), it is not possible to determine the association constant (K_a) due to going beyond the linearity of concentration determination. Despite the fact that luminescence quenching was also observed for the **SIPEC-1**/DAPI system, it is problematic to determine the K_a ; SDS contributes to this system, the addition of which to DAPI causes an increase in luminescence. Therefore, the next step is the quantitative characteristics of the interaction of the dye with Pillar[5]arene **2** and **SIPEC-2**. In the luminescence spectrum of pure DAPI (Figure 8a), four main emission bands can be distinguished at 422, 450, 495, and 560 nm. When DAPI interacts with Pillar[5]arene **2**, a nonequivalent change in intensity is observed at bands 422, 450, and 495 nm (Figure 8b). This can be seen more clearly when plotting graphs in the I/I_0 format (Figure 8c), where I_0 is the intensity of DAPI emission in the absence of a macrocycle **2**. Thus, for the **2**/DAPI system, three independent emission regions can be distinguished, which indicate the existence of three types of particles with emission in different spectral regions.

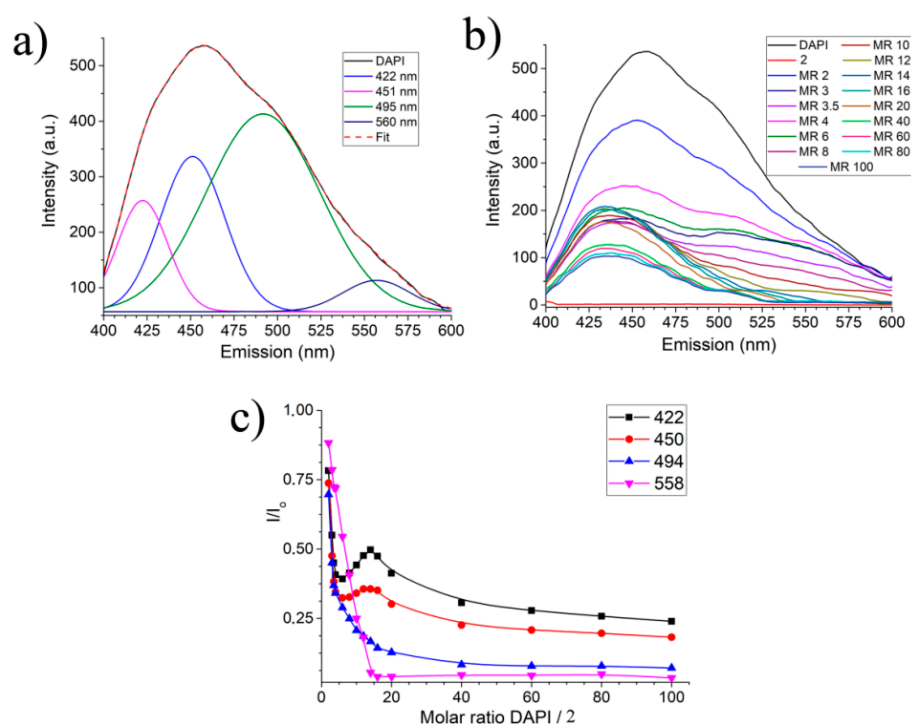


Figure 8. (a) DAPI luminescence spectrum with deconvolution of emission band (RMSE = 0.9996); (b) titration of DAPI by compound **2** indicating molar ratios $c_m(\text{DAPI})/c_m(\mathbf{2})$; (c) titration of DAPI by compound **2** in I/I_0 format at different emission wavelengths.

To prove that associates of different compositions luminesce in different regions of the spectrum, the analysis of supramolecular aggregates was carried out by the NTA method. Nanosight LM-10 allows to cut off luminescent particles using extinguishing filters. Figure 9 shows the dependence of the size and concentration of nanoparticles in a solution without a luminescence quenching filter (Figure 9a), namely, all particles that are present in the solution. There is also luminescence spectrum of DAPI and DAPI/**2** at a molar ratio of 1:1, which is given for visual display of the type of luminescent nanoparticles (Figure 9c). The average size of all particles in the system is 173 ± 5 nm with a total amount of 12.1×10^8 particles/mL (Figure 9a). A significant decrease in concentration and an increase in the size of the detected particles are observed when using a cutoff filter at 430 nm (Figure 9b).

After using cutoff filters at 430 and 500 nm (Figure 9b,d), the average hydrodynamic particle diameter changes to 244 ± 15 and 203 ± 30 nm, respectively. The increase in error is primarily due to a decrease in signal intensity. It is worth noting that when using a cutoff filter at 430 nm, the particles that we observe when using a 500 nm filter are also recorded. The subsequent study of the **2**/DAPI system at other molar ratios showed that an increase in the content of Pillar[5]arene **2** leads to the normalization and stabilization of the type of luminescent particles. When the molar ratio **2**/DAPI is more than three, there is only one type of luminescent particles in the system in the entire range (Table S5, Figure S11).

Based on the data obtained, it can be assumed that with an increase in the concentration of **2**, associates of a complex composition are first formed, consisting of DAPI associates and associates of macrocycle **2**. A further increase in the concentration of Pillar[5]arene **2** leads to the destruction of self-associates of the dye and their interaction with the **2**, while maintaining the luminescence of the dye. A significant excess of compound **2** leads to complete solubilization of DAPI with quenching of luminescence [73,74].

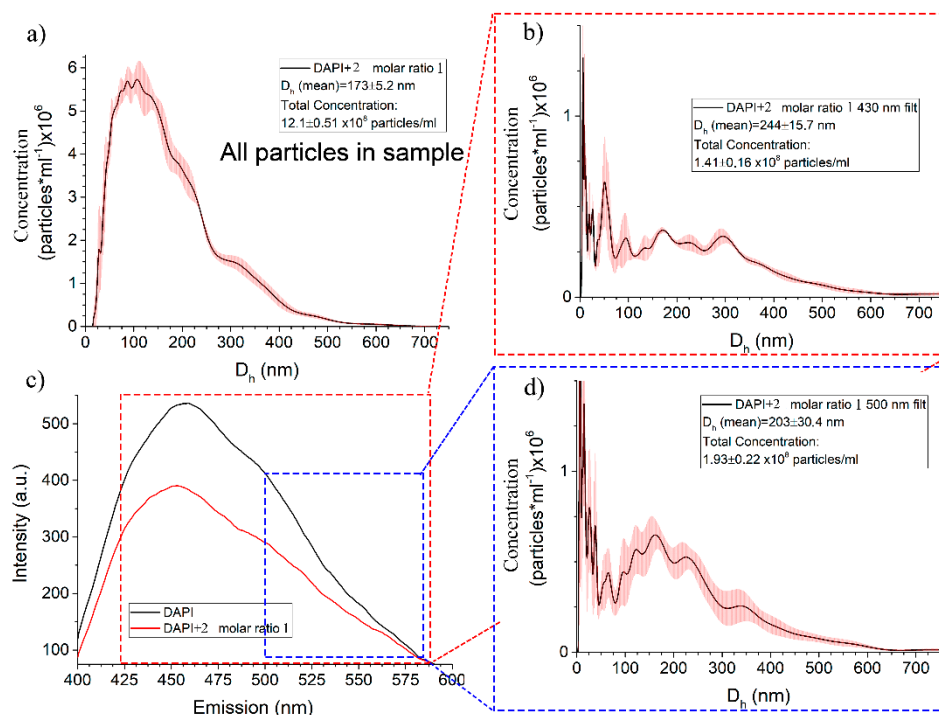


Figure 9. (a) Dependence of the concentration of particles on their size in a DAPI/2 solution at a 1:1 molar ratio; (b) Dependence of the concentration of particles on their size in a solution of DAPI/2 at a 1:1 molar ratio using a cutoff filter at 430 nm; (c) Luminescence spectrum of DAPI ($c = 3 \times 10^{-5}$ M) and DAPI/2 at a 1:1 molar ratio; (d) Dependence of the concentration of particles on their size in a solution of DAPI/2 at a 1:1 molar ratio using a cutoff filter at 500 nm.

This assumption is confirmed (Figure 10a, Table 1) when processing the results obtained by the method of construction of a Scatchard plot [75].

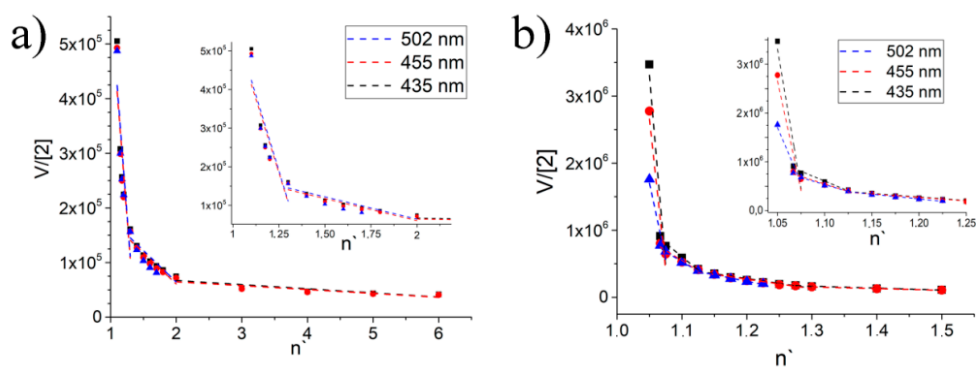


Figure 10. Determination of linearity sections using the Scatchard method: (a) relative to the equilibrium concentration of Pillar[5]arene 2; (b) relative to the equilibrium concentration of macrocycle 2 in SIPEC-2/DAPI system.

Table 1. Calculated K_{it} for the 2/DAPI and SIPEC-2/DAPI systems.

K_a	Emission 2/DAPI			Emission SIPEC-2/DAPI		
	435 nm	455 nm	500 nm	435 nm	455 nm	500 nm
1	1.56×10^6	1.52×10^6	1.50×10^6	1.14×10^8	8.98×10^8	4.52×10^8
2	1.15×10^5	1.14×10^5	1.15×10^5	7.69×10^6	6.11×10^6	5.73×10^6
3	7.57×10^3	7.08×10^3	N/A	1.43×10^6	1.41×10^6	1.94×10^6
4	N/A	N/A	N/A	2.89×10^5	2.42×10^5	N/A

N/A: not applicable.

As seen in Figure 10 in the 2/DAPI system, there are three linearity sections (Figure 10a), and in the SIPEC-2/DAPI there are four linearity sections (Figure 10b) from which it follows that the systems have three and four association constants, respectively. For the 2/DAPI system, we attribute the first association constant to the interaction of compound 2 with its own associate DAPI, since it is in excess. The second constant refers to the true constant of association of individual DAPI molecules with compound 2. The third constant we refer to is the constant of association of the supramolecular aggregate 2/DAPI with free molecules of compound 2 along the perimeter. That is why there is no signal in the luminescence spectrum at a wavelength of 500 nm, and consequently, it is impossible to calculate the interaction constant (Table 1).

When switching to the SIPEC-2/DAPI system, we observe, first, a general increase in the values of the association constants in the system, and second, an additional association constant. Both effects are explained by the presence of surfactants in the system at a concentration above the critical micelle concentration (CMC) point. That is, the first constant with the maximum energy refers to the solubilization of the dye into the micelle. The subsequent association constants refer to the same processes as in the 2/DAPI system. The overall increase in the constant value by an order of magnitude or more is explained by the facilitation of the interaction of DAPI and 2 due to the effect of concentration in the micelle. The fact that the association of constants in the SIPEC-2/DAPI system to the same processes is confirmed by the absence of the fourth association constant at a wavelength of 500 nm.

3. Materials and Methods

3.1. General

All chemicals were purchased from Acros (Fair Lawn, NJ, USA), and most of them were used as received without additional purification. Organic solvents were purified by standard procedures. ^1H NMR spectrum was obtained on a Bruker Avance-400 spectrometer (Bruker Corp., Billerica, MA, USA) (^1H 400 MHz). Chemical shifts were determined against the signals of residual protons of deuterated solvent (D_2O , $\text{DMSO-}d_6$). The concentrations of the compounds were equal to 3–5% in all the records. Melting points were determined using Boetius Block apparatus (VEB Kombinat Nagema, Radebeul, Germany). UV-vis spectra were recorded on a Shimadzu UV-3600 spectrometer (Kyoto, Japan). All the aqueous solutions were prepared with the Millipore-Q deionized water ($> 18.0 \text{ M}\Omega \text{ cm}$ at 25°C). The size, concentration and movement of nanoparticles were determined using a NanoSight LM10 instrument (Malvern Instruments Ltd., UK) equipped with a C11440-50B CMOS camera with an FL-280 scientific image sensor (Hamamatsu Photonics, Japan) as a detector. Luminescence spectra were recorded on a Perkin Elmer LS 55 (Perkin Elmer, Waltham, MA, USA).

4,8,14,18,23,26,28,31,32,35-Decakis-[(N-(3',3',3'-trimethylammoniumpropyl)carbamoylmethoxy)Pillar[5]arene decaiodide (1) was prepared by a literature method [76].

4,8,14,18,23,26,28,31,32,35-Deca(carboxymethoxy)Pillar[5]arene tributylammonium salt (2) was prepared by a literature method [77].

3.2. UV-Vis Spectroscopy

Absorption spectra were recorded on a Shimadzu UV-3600 spectrometer (Kyoto, Japan). Quartz cuvettes with an optical path length of 10 mm were used. Deionized water was used for preparation of the solutions. Absorption spectra of mixtures were recorded after 1 h incubation at 20°C . Solutions of SDS and DTAC were added to those of compounds 1, 2 ($3 \times 10^{-5} \text{ M}$) in a 1:10 ratio to study the complexation of Pillar[5]arenes with guests in solvent.

3.2.1. Determination of the Stability Constant and Stoichiometry of the Complex by Spectrophotometric Titration

A 3×10^{-3} M solution of SDS (DTAC) (30, 60, 90, 120, 150, 180, 210, 240, 270 and 300 μ L) in water was added to 0.3 mL of a solution of **1** (**2**) (3×10^{-4} M) in water and diluted to a final volume of 3 mL with water. The UV spectra of the solutions were then recorded. The stability constant of complex was calculated by Bindfit [66]. Three independent experiments were carried out for each series.

3.2.2. Job Plots

Job Plots for hosts **1** and **2** and guests SDS and DTAC were determined in deionized water with the ratio varied from 0.6:2.4 to 2.4:0.6. Each of the measurements of the series was performed three times.

3.3. Dynamic Light Scattering (DLS)

3.3.1. Particles' Size

The Zetasizer Nano ZS instrument (Worcestershire, UK) equipped with the 4 mW He-Ne laser (633 nm) was used for the determination of particle size. Measurements were performed at a detection angle of 173° and the software automatically determined the measurement position within the quartz cuvette. Processing of the results was performed by the DTS program (Dispersion Technology Software 4.20). Deionized water was used to prepare the solutions. The concentrations of the compounds **1** and **2** were 1×10^{-6} M, 1×10^{-5} M, 1×10^{-4} M, and 1×10^{-3} M. The particle sizes were measured after 1 h mixing. To study the aggregation of Pillar[5]arenes with surfactants, water solutions of SDS and DTAC were added to the solution of compounds **1** and **2** ($1 \times 10^{-3} \div 1 \times 10^{-6}$ M) in chloroform at 1:1, 1:10, 1:100, and 1:1000 ratios. The particle sizes were measured after 1 h mixing. Measurements were determined after 24 and 178 h three times to evaluate kinetic stability.

3.3.2. Zeta Potentials

Zeta (ζ) potentials were measured on a Zetasizer Nano ZS from Malvern Instruments (Worcestershire, UK). Samples were prepared as for the DLS measurements and were transferred with the syringe to the disposable folded capillary cell for measurement. The zeta potentials were measured using the Malvern M3-PALS method and averaged from three measurements.

3.4. Luminescence Spectroscopy

Luminescence spectra were recorded on a Perkin Elmer LS 55 (Perkin Elmer, Waltham, MA, USA) at an excitation wavelength of 358 nm (excitation gap—3 nm) and emission scan range of 400–600 nm (emission gap—7 nm), the gain of the photo detector was 650 V, the scanning speed was 250 nm per minute. Quartz cuvettes with an optical path length of 10 mm were used. The cuvette was located in the front face position. Deionized water was used for preparation of the solutions. Absorption spectra of mixtures were recorded after 1 h incubation at 20 °C. Excitation and emission slits were equal to 2 nm for DAPI in the presence of Pillar[5]arenes **1** and **2** and to 1 nm in the presence of DTAC and SDS. The fluorescence spectra were recorded with the 3×10^{-5} M concentration for DAPI. The concentration of the DAPI was determined individually by 3 wavelengths by the Beer–Lambert law method according to the linear section of the intensity variation, in the range of dye concentration from 3×10^{-5} to 5×10^{-6} M.

3.5. Nanoparticle Tracking Analysis (NTA)

The size, concentration and movement of nanoparticles were determined using a NanoSight LM10 instrument (Malvern Instruments Ltd., Worcestershire, UK) equipped with a C11440-50B CMOS camera with an FL-280 scientific image sensor (Hamamatsu Photonics, Hamamatsu, Japan) as a detector. Measurements were carried out in a special

cell for organic solvents with a modified angle of entry of the laser beam into the solution, a 405 nm laser (version cd, S/N 2990491) and a Kalrez sealing ring. An HH804 contact thermometer (Omega Engineering, Inc., Stamford, CT, USA) was used to determine the temperature in the cell throughout the experiment. NanoSight NTA 2.3 software (build 0033) was used to process the results.

Video recording of the samples was carried out in a constant flow of liquid, for greater statistics. The dosing rate was 10 $\mu\text{L}/\text{min}$. From 3 to 5 video recordings were recorded, from 30 to 240 s long, depending on the number of particles in the solution. The first measurements to fix all visible particles in the solution were carried out without an extinguishing filter, followed by a cutoff filter at 430 nm and 500 nm. Thus, particles with emissivity were recorded at wavelengths of more than 430 and 500 nm, respectively.

3.6. Molecular Docking

DINC 2.0 web server [71,72] was used to study molecular interactions between Pillar[5]arene 2 and ligand (DAPI). DINC is a parallelized meta-docking method for the incremental docking of ligands. The strategy of DINC involves incrementally docking overlapping fragments with a growing number of atoms, while maintaining the number of flexible bonds constant during this incremental process [72]. The grid size was set to $\sim 30 \text{ \AA} \times 30 \text{ \AA} \times 30 \text{ \AA}$ xyz points and grid center was designated at dimensions (x, y, and z): 0.8, 0.8, and -6.4 .

4. Conclusions

Thus, the novel self-assembling systems based on oppositely charged Pillar[5]arenes and surfactants for encapsulation of dye DAPI were created. The aggregation behavior of macrocycles synthesized and surfactants in the presence of Pillar[5]arenes functionalized by carboxy and ammonium terminal groups were studied using the set physical methods. It was shown that by varying the molar ratio in Pillar[5]arene-surfactant systems, it is possible to obtain various types of nanosystems: (1) host-guest complexes at equimolar ratio of Pillar[5]arene-surfactant and (2) interpolyelectrolyte complexes (IPECs), are self-assembled materials formed in aqueous medium by two oppositely charged polyelectrolytes (macrocycle and surfactant micelles). It has been suggested that interaction of Pillar[5]arenes with surfactants is predominantly driven by cooperative electrostatic interactions. Synthesized stoichiometric and non-stoichiometric IPECs specifically interact with a third component, imaging system agent, 4',6-diamidino-2-phenylindole (DAPI). UV-vis, luminescent spectroscopy and molecular docking data show the structural feature of dye-loaded IPEC and key role of the electrostatic, π - π -stacking, cation- π interactions in their formation. The nanoparticle trajectory analysis detected that the use of IPEC formed by surfactants and Pillar[5]arenes leads to an increase in the association constant, which is responsible for the complete binding of the dye. This work elucidated the mechanism of self-assembly between Pillar[5]arenes and surfactants, providing additional information on features of dye-loaded IPEC and the key role of the electrostatic, π - π -stacking, cation- π interactions in their formation. Design of dye-loaded supramolecular Pillar[5]arene-surfactant systems will certainly be in demand in pharmaceuticals and biomedical diagnostics.

Supplementary Materials: The following are available online at <https://www.mdpi.com/article/10.3390/ijms22116038/s1>.

Author Contributions: Conceptualization, writing—review and editing, supervision, I.S.; investigation, writing—original draft preparation and visualization, A.N.; investigation, data curation, editing, supervision, L.Y.; software, A.B.; software and editing, A.K. All authors have read and agreed to the published version of the manuscript.

Funding: The work was supported by the Russian Science Foundation (Grant No. 18-73-10094).

Acknowledgments: The investigation of the compounds by luminescence spectroscopy was carried out within the framework of the grants of the President of the Russian Federation for state support of young Russian scientists—candidates of sciences and leading scientific schools of Russian Federation

(MK-723.2021.1.3, NSh-2499.2020.3). The authors are grateful to the staff of the Spectral-Analytical Center in the Shared Facilities for the Study of Structure, Composition and Properties of Substances and Materials at the A.E. Arbutov Institute of Organic and Physical Chemistry of the Kazan Scientific Center of the Russian Academy of Sciences for their assistance and helpful discussion.

Conflicts of Interest: The authors declare no conflict of interest. The funders had no role in the design of the study; in the collection, analyses, or interpretation of data; in the writing of the manuscript, or in the decision to publish the results.

References

1. Yang, X.; Yuan, D.; Hou, J.; Sedgwick, A.C.; Xu, S.; James, T.D.; Wang, L. Organic/inorganic supramolecular nano-systems based on host/guest interactions. *Coordin. Chem. Rev.* **2021**, *428*, 213609. [[CrossRef](#)]
2. Hoque, J.; Sangaj, N.; Varghese, S. Stimuli-responsive supramolecular hydrogels and their applications in regenerative medicine. *Macromol. Biosci.* **2018**, *19*, 1800259. [[CrossRef](#)]
3. Yin, H.; Zhang, X.; Wei, J.; Lu, S.; Bardelang, D.; Wang, R. Recent advances in supramolecular antidotes. *Theranostics* **2021**, *11*, 1513–1526. [[CrossRef](#)]
4. Nazarova, A.; Shurpik, D.; Padnya, P.; Mukhametzyanov, T.; Cragg, P.; Stoikov, I. Self-assembly of supramolecular architectures by the effect of amino acid residues of quaternary ammonium Pillar[5]arenes. *Int. J. Mol. Sci.* **2020**, *21*, 7206. [[CrossRef](#)]
5. Kaizerman-Kane, D.; Hadar, M.; Joseph, R.; Logviniuk, D.; Zafrani, Y.; Fridman, M.; Cohen, Y. Design guidelines for cationic pillar[n]arenes that prevent biofilm formation by gram-positive pathogens. *CS Infect. Dis.* **2021**, *7*, 579–585.
6. Nazarova, A.A.; Yakimova, L.S.; Padnya, P.L.; Evtugyn, V.G.; Osin, Y.N.; Fragg, P.J.; Stoikov, I.I. Monosubstituted Pillar[5]arene functionalized with (amino)phosphonate fragments are “smart” building blocks for constructing nanosized structures with some s- and p-metal cations in the organic phase. *New J. Chem.* **2019**, *43*, 14450–14458. [[CrossRef](#)]
7. Zhu, H.; Liu, J.; Shi, B.; Wang, H.; Mao, Z.; Shan, T.; Huang, F. Pillar[5]arene-based host-guest recognition facilitated magnetic separation and enrichment of cell membrane proteins. *Mater. Chem. Front.* **2018**, *2*, 1475–1480. [[CrossRef](#)]
8. Yue, L.; Yang, K.; Lou, X.-Y.; Yang, Y.-W.; Wang, R. Versatile roles of macrocycles in organic-inorganic hybrid materials for biomedical applications. *Matter* **2020**, *3*, 1557–1588. [[CrossRef](#)]
9. Yakimova, L.S.; Shurpik, D.N.; Makhmutova, A.R.; Stoikov, I.I. Pillar[5]arenes bearing amide and carboxylic groups as synthetic receptors for alkali metal ions. *Macroheterocycles* **2017**, *10*, 226–232. [[CrossRef](#)]
10. Lan, S.; Liu, Y.; Shi, K.; Ma, D. Acetal-functionalized Pillar[5]arene: A pH-responsive and versatile nanomaterial for the delivery of chemotherapeutic agents. *ACS Appl. Bio Mater.* **2020**, *3*, 2325–2333. [[CrossRef](#)]
11. Cao, Y.; Chen, Y.; Zhang, Z.; Wang, J.; Yuan, X.; Zhao, Q.; Ding, Y.; Yao, Y. CO₂ and photo-controlled reversible conversion of supramolecular assemblies based on water soluble Pillar[5]arene and coumarin-containing guest. *Chin. Chem. Lett.* **2021**, *32*, 349–352. [[CrossRef](#)]
12. Fernando, A.; Mako, T.L.; Levenson, A.M.; Cesana, P.T.; Mendieta, A.M.; Racicot, J.M.; DeBoef, B.; Levine, M. A polycationic Pillar[5]arene for the binding and removal of organic toxicants from aqueous media. *Supramol. Chem.* **2019**, *31*, 545–557. [[CrossRef](#)]
13. Nazarova, A.A.; Shibaeva, K.S.; Stoikov, I.I. Synthesis of the monosubstituted Pillar[5]arenes with 1-aminophosphonate fragment. *Phosphorus Sulfur* **2016**, *191*, 1583–1584. [[CrossRef](#)]
14. Chao, S.; Lu, X.; Ma, N.; Shen, Z.; Zhang, F.; Pei, Y.; Pei, Z. A supramolecular nanoprodruge based on a boronate ester linked curcumin complexing with water-soluble Pillar[5]arene for synergistic chemotherapies. *Chem. Commun.* **2020**, *56*, 8861–8864. [[CrossRef](#)] [[PubMed](#)]
15. Chang, Y.; Chen, J.-Y.; Wei, L.; Yang, J.; Lin, T.; Zeng, L.; Xu, J.-F.; Hou, J.-L.; Zhang, X. Targeting the cell membrane by charge-reversal amphiphilic pillar[5]arene for the selective killing of cancer cells. *ACS Appl. Mater. Interfaces* **2019**, *11*, 38497–38502. [[CrossRef](#)] [[PubMed](#)]
16. Nazarova, A.A.; Yakimova, L.S.; Klochkov, V.V.; Stoikov, I.I. Monoaminophosphorylated Pillar[5]arenes as hosts for alkaneamines. *New J. Chem.* **2017**, *41*, 1820–1826. [[CrossRef](#)]
17. Zhu, H.; Li, Q.; Gao, Z.; Wang, H.; Shi, B.; Wu, Y.; Shangguan, L.; Hong, X.; Wang, F.; Huang, F. Pillar[5]arene host-guest complexation induced chirality amplification: A new way to detect cryptochiral compounds. *Angew. Chem. Int. Ed.* **2020**, *59*, 10868–10872. [[CrossRef](#)] [[PubMed](#)]
18. Chen, L.; Cai, Y.; Feng, W.; Yuan, L. Pillar[5]arenes as macrocyclic hosts: A rising star in metal ion separation. *Chem. Commun.* **2019**, *55*, 7883–7898. [[CrossRef](#)]
19. Li, Q.; Zhu, H.; Huang, F. Pillar[5]arene-based supramolecular functional materials. *Trends Chem.* **2020**, *2*, 850–864. [[CrossRef](#)]
20. Yu, G.; Chen, X. Host-guest chemistry in supramolecular theranostics. *Theranostics* **2019**, *9*, 3041–3074. [[CrossRef](#)]
21. Liu, Y.; Zhang, Y.; Zhu, H.; Wang, H.; Tian, W.; Shi, B. A supramolecular hyperbranched polymer with multi-responsiveness constructed by Pillar[5]arene-based host-guest recognition and its application in the breath figure method. *Mater. Chem. Front.* **2018**, *2*, 1568–1573. [[CrossRef](#)]
22. Zhang, H.; Liu, Z.; Zhao, Y. Pillar[5]arene-based self-assembled amphiphiles. *Chem. Soc. Rev.* **2018**, *47*, 5491–5528. [[CrossRef](#)] [[PubMed](#)]
23. Jie, K.; Zhou, Y.; Yao, Y.; Shi, B.; Huang, F. CO₂-responsive Pillar[5]arene-based molecular recognition in water: Establishment and application in gas-controlled self-assembly and release. *J. Am. Chem. Soc.* **2015**, *137*, 10472–10475. [[CrossRef](#)] [[PubMed](#)]

24. Wei, T.; Li, H.; Zhu, Y.; Lu, T.; Shi, B.; Lin, Q.; Yao, H.; Zhang, Y. CoPillar[5]arene-based supramolecular polymer gel: Controlling stimuli–response properties through a novel strategy with surfactant. *RSC Adv.* **2015**, *5*, 60273–60278. [[CrossRef](#)]
25. Ma, Y.; Ji, X.; Xiang, F.; Chi, X.; Han, C.; He, J.; Abliz, Z.; Chen, W.; Huang, F. A cationic water-soluble Pillar[5]arene: Synthesis and host–guest complexation with sodium 1-octanesulfonate. *Chem. Commun.* **2011**, *47*, 12340–12342. [[CrossRef](#)]
26. Silveira, E.V.; Nascimento, V.; Wanderlind, E.H.; Affeldt, R.F.; Micke, G.A.; Garcia-Rio, L.; Nome, F. Inhibitory and cooperative effects regulated by pH in host–guest complexation between cationic Pillar[5]arene and reactive 2-carboxyphthalanilic acid. *J. Org. Chem.* **2019**, *84*, 9684–9692. [[CrossRef](#)]
27. Zhang, D.; Cheng, J.; Wei, L.; Song, W.; Wang, L.; Tang, H.; Cao, D. Host-guest complexation of monoanionic and dianionic guests with a polycationic Pillar[5]arene host: Same two-step mechanism but striking difference in rate upon inclusion. *J. Phys. Chem. Lett.* **2020**, *11*, 2021–2026. [[CrossRef](#)]
28. Shurpik, D.N.; Makhmutova, L.I.; Usachev, K.S.; Islamov, D.R.; Mostovaya, O.A.; Nazarova, A.A.; Kiznyaev, V.N.; Stoikov, I.I. Towards universal stimuli-responsive drug delivery systems: Pillar[5]arenes synthesis and self-assembly into nanocontainers with tetrazole polymers. *Nanomaterials* **2021**, *11*, 947. [[CrossRef](#)]
29. Wang, R.; Sun, Y.; Zhang, F.; Song, M.; Tian, D.; Li, H. Temperature-sensitive artificial channels through Pillar[5]arene-based host–guest interactions. *Angew. Chem. Int. Ed.* **2017**, *56*, 5294–5298. [[CrossRef](#)] [[PubMed](#)]
30. Ogoshi, T.; Suetto, R.; Yoshikoshi, K.; Sakata, Y.; Akine, S.; Yamagishi, T.-A. Host–guest complexation of perethylated Pillar[5]arene with alkanes in the crystal state. *Angew. Chem. Int. Ed.* **2015**, *54*, 9849–9852. [[CrossRef](#)]
31. Cao, D.; Meier, H. Pillar[5]arene-based fluorescent sensors for the tracking of organic compounds. *Chinese Chem. Lett.* **2019**, *30*, 1758–1766. [[CrossRef](#)]
32. Feng, W.; Jin, M.; Yang, K.; Pei, Y.; Pei, Z. Supramolecular delivery systems based on Pillar[5]arenes. *Chem. Commun.* **2018**, *54*, 13626–13640. [[CrossRef](#)] [[PubMed](#)]
33. Shao, L.; Pan, Y.; Hua, B.; Xu, S.; Yu, G.; Wang, M.; Liu, B.; Huang, F. Constructing adaptive photosensitizers via supramolecular modification based on Pillar[5]arene host–guest interactions. *Angew. Chem. Int. Ed.* **2020**, *59*, 11779–11783. [[CrossRef](#)]
34. Gómez-González, B.; Francisco, V.; Montecinos, R.; García-Río, L. Investigation of the binding modes of a positively charged Pillar[5]arene: Internal and external guest complexation. *Org. Biomol. Chem.* **2017**, *15*, 911–919. [[CrossRef](#)]
35. Yang, K.; Pei, Y.; Wen, J.; Pei, Z. Recent advances in pillar[n]arenes: Synthesis and applications based on host–guest interactions. *Chem. Commun.* **2016**, *52*, 9316–9326. [[CrossRef](#)]
36. Yakimova, L.; Vavilova, A.; Shibaeva, K.; Sultanaev, V.; Mukhametzyanov, T.; Stoikov, I. Supramolecular approaches to the formation of nanostructures based on phosphonate-thiacalix[4]arenes, their selective lysozyme recognition. *Colloid. Surface Asp.* **2021**, *611*, 125897. [[CrossRef](#)]
37. Kashapov, R.; Gaynanova, G.; Gabdrakhmanov, D.; Kuznetsov, D.; Pavlov, R.; Petrov, K.; Zakharova, L.; Sinyashin, O. Self-assembly of amphiphilic compounds as a versatile tool for construction of nanoscale drug carriers. *Int. J. Mol. Sci.* **2020**, *21*, 6961. [[CrossRef](#)] [[PubMed](#)]
38. Li, Q.; Li, X.; Ning, L.; Tan, C.-H.; Mu, Y.; Wang, R. Hyperfast water transport through biomimetic nanochannels from peptide-attached (pR)-Pillar[5]arene. *Small* **2019**, *15*, 1804678. [[CrossRef](#)] [[PubMed](#)]
39. Yakimova, L.; Padnya, P.; Tereshina, D.; Kunafina, A.; Nugmanova, A.; Osin, Y.; Evtugyn, V.; Stoikov, I. Interpolyelectrolyte mixed nanoparticles from anionic and cationic thiocalix[4]arenes for selective recognition of model biopolymers. *J. Mol. Liq.* **2019**, *279*, 9–17. [[CrossRef](#)]
40. Kashapov, R.; Razuvayeva, Y.; Ziganshina, A.; Sergeeva, T.; Lukashenko, S.; Sapunova, A.; Voloshina, A.; Kashapova, N.; Nizameev, I.; Salnikov, V.; et al. Supraamphiphilic systems based on metallosurfactant and calix[4]resorcinol: Self-assembly and drug delivery potential. *Inorg. Chem.* **2020**, *59*, 18276–18286. [[CrossRef](#)] [[PubMed](#)]
41. Rui, L.; Liu, L.; Wang, Y.; Gao, Y.; Zhang, W. Orthogonal approach to construct cell-like vesicles via Pillar[5]arene-based amphiphilic supramolecular polymers. *ACS Macro Lett.* **2016**, *5*, 112–117. [[CrossRef](#)]
42. Concellón, A.; Romero, P.; Marcos, M.; Barberá, J.; Sánchez-Somolinos, C.; Mizobata, M.; Ogoshi, T.; Serrano, J.L.; Barrio, J. Coumarin-containing Pillar[5]arenes as multifunctional liquid crystal macrocycles. *J. Org. Chem.* **2020**, *85*, 8944–8951. [[CrossRef](#)] [[PubMed](#)]
43. Sharma, V.S.; Shah, A.P.; Sharma, A.S. A new class of supramolecular liquid crystals derived from azo calix[4]arene functionalized 1,3,4-thiadiazole derivatives. *New J. Chem.* **2019**, *43*, 3556–3564. [[CrossRef](#)]
44. Padnya, P.L.; Andreyko, E.A.; Gorbatova, P.A.; Parfenov, V.V.; Rizvanov, I.K.; Stoikov, I.I. Towards macrocyclic ionic liquids: Novel ammonium salts based on tetrasubstituted p-tert-butylthiacalix[4]arenes. *RSC Adv.* **2017**, *7*, 1671–1686. [[CrossRef](#)]
45. Kashapov, R.; Lykova, A.; Kashapova, N.; Ziganshina, A.; Sergeeva, T.; Sapunova, A.; Voloshina, A.; Zakharova, L. Nanoencapsulation of food bioactives in supramolecular assemblies based on cyclodextrins and surfactant. *Food Hydrocoll.* **2021**, *113*, 106449. [[CrossRef](#)]
46. Wang, J.; Ding, X.; Guo, X. Assembly behaviors of calixarene-based amphiphile and supraamphiphile and the applications in drug delivery and protein recognition. *Adv. Colloid Interface Sci.* **2019**, *269*, 187–202. [[CrossRef](#)]
47. Hu, X.-Y.; Gao, L.; Mosel, S.; Ehlers, M.; Zellerman, E.; Jiang, H.; Knauer, S.K.; Wang, L.; Schmuck, C. From supramolecular vesicles to micelles: Controllable construction of tumor-targeting nanocarriers based on host–guest interaction between a Pillar[5]arene-based prodrug and a RGD-sulfonate guest. *Small* **2018**, *14*, 1803952. [[CrossRef](#)] [[PubMed](#)]

48. Lv, X.; Xia, D.; Zuo, Y.; Wu, X.; Wei, X.; Wang, P. Gemini-type supramolecular amphiphile based on a water-soluble Pillar[5]arene and an azastilbene guest and its application in stimuli-responsive self-assemblies. *Langmuir* **2019**, *35*, 8383–8388. [CrossRef] [PubMed]
49. Morohashi, N.; Hattori, T. Selective guest inclusion by crystals of calixarenes: Potential for application as separation materials. *J. Incl. Phenom. Macro.* **2018**, *90*, 261–277. [CrossRef]
50. Baldini, L.; Casnati, A.; Sansone, F. Multivalent and multifunctional calixarenes in bionanotechnology. *Eur. J. Org. Chem.* **2020**, *2020*, 5056–5069. [CrossRef]
51. Das, D.; Assaf, K.I.; Nau, W.M. Applications of cucurbiturils in medicinal chemistry and chemical biology. *Front. Chem.* **2019**, *7*, 619. [CrossRef] [PubMed]
52. Vasilieva, E.A.; Valeeva, F.G.; Yeliseeva, O.E.; Lukashenko, S.S.; Saifutdinova, M.N.; Zakharov, V.M.; Gavrilova, E.L.; Zakharova, L.Y. Supramolecular nanocontainers based on hydrophobized calix[4]resorcinol: Modification by gemini surfactants and polyelectrolyte. *Macroheterocycles* **2017**, *10*, 182–189. [CrossRef]
53. García-Río, L.; Basilio, N. Supramolecular surfactants derived from calixarenes. *Curr. Opin. Colloid Interface Sci.* **2019**, *44*, 225–237. [CrossRef]
54. Shalaeva, Y.V.; Morozova, J.E.; Syakaev, V.V.; Kazakova, E.K.; Ermakova, A.M.; Nizameev, I.R.; Kadirov, M.K.; Konovalov, A.I. Supramolecular nanoscale systems based on amphiphilic tetramethylsulfonatocalix[4]resorcinarenes and cationic polyelectrolyte with controlled guest molecule binding. *Supramol. Chem.* **2017**, *29*, 278–289. [CrossRef]
55. Gallego-Yerga, L.; Posadas, I.; de la Torre, C.; Ruiz-Almansa, J.; Sansone, F.; Mellet, C.O.; Casnati, A.; García Fernández, J.M.; Ceña, V. Docetaxel-loaded nanoparticles assembled from β -cyclodextrin/calixarene giant surfactants: Physicochemical properties and cytotoxic effect in prostate cancer and glioblastoma cells. *Front. Pharmacol.* **2017**, *8*, 249. [CrossRef]
56. Hasan, M.Z.; Mahbub, S.; Hoque, M.A.; Rub, M.A.; Kumar, D. Investigation of mixed micellization study of sodium dodecyl sulfate and tetradecyltrimethylammonium bromide mixtures at different compositions: Effect of electrolytes and temperatures. *J. Phys. Org. Chem.* **2020**, *33*, e4047. [CrossRef]
57. Tan, Z.; Jiang, Y.; Zhang, W.; Karls, L.; Lodge, T.P.; Reineke, T.M. Polycation architecture and assembly direct successful gene delivery: Micelleplexes outperform polyplexes via optimal DNA packaging. *J. Am. Chem. Soc.* **2019**, *141*, 15804–15817. [CrossRef] [PubMed]
58. Palena, M.C.; García, M.C.; Manzo, R.H.; Jimenez-Kairuz, A.F. Self-organized drug-interpolyelectrolyte nanocomplexes loaded with anionic drugs. Characterization and in vitro release evaluation. *J. Drug Deliv. Sci. Tec.* **2015**, *30*, 45–53. [CrossRef]
59. Korzhikov-Vlakh, V.; Katernuk, I.; Pilipenko, I.; Lavrentieva, A.; Guryanov, I.; Sharoyko, V.; Manshina, A.A.; Tennikova, T.B. Photosensitive poly-L-lysine/heparin interpolyelectrolyte complexes for delivery of genetic drugs. *Polymers* **2020**, *12*, 1077. [CrossRef] [PubMed]
60. Basilio, N.; Gómez, B.; Garcia-Río, L.; Francisco, V. Using calixarenes to model polyelectrolyte surfactant nucleation sites. *Chem. Eur. J.* **2013**, *19*, 4570–4576. [CrossRef]
61. Nazarova, A.A.; Makhmutova, L.I.; Stoikov, I.I. Synthesis of Pillar[5]arenes with a PH-containing fragment. *Russ. J. Gen. Chem.* **2017**, *87*, 1941–1945. [CrossRef]
62. Kashapov, R.; Razuvayeva, Y.; Ziganshina, A.; Sergeeva, T.; Kashapova, N.; Sapunova, A.; Voloshina, A.; Nizameev, I.; Salnikov, V.; Zakharova, L. Supramolecular assembly of calix[4]resorcinarenes and chitosan for the design of drug nanocontainers with selective effects on diseased cells. *New J. Chem.* **2020**, *44*, 17854–17863. [CrossRef]
63. Nicolas, H.; Yuan, B.; Xu, J.; Zhang, X.; Schönhoff, M. pH-responsive host-guest complexation in pillar[6]arene-containing polyelectrolyte multilayer films. *Polymers* **2017**, *9*, 719. [CrossRef] [PubMed]
64. Kapuscinski, J.; Skoczylas, B. Fluorescent complexes of DNA with DAPI 4'-6-diamidine-2-phenyl indole 2HCl or DC14'-6-dicarboxyamide-2-phenyl indole. *Nucleic Acids Res.* **1978**, *5*, 3775–3799. [CrossRef]
65. Biancardi, A.; Biver, T.; Secco, F.; Mennucci, B. An investigation of the photophysical properties of minor groove bound and intercalated DAPI through quantum-mechanical and spectroscopic tools. *Phys. Chem. Chem. Phys.* **2013**, *15*, 4596–4603. [CrossRef] [PubMed]
66. Bindfit v0.5. Available online: <http://supramolecular.org/bindfit> (accessed on 29 April 2021).
67. Kramarenko, E.Y.; Khokhlov, A.R.; Reineker, P. Stoichiometric polyelectrolyte complexes of ionic block copolymers and oppositely charged polyions. *J. Chem. Phys.* **2006**, *125*, 194902. [CrossRef] [PubMed]
68. Burova, T.V.; Grinberg, N.V.; Dubovik, A.S.; Olenichenko, E.A.; Orlov, V.N.; Grinberg, V.Y. Interpolyelectrolyte complexes of lysozyme with short poly[di(carboxylatophenoxy)phosphazene]. Binding energetics and protein conformational stability. *Polymer* **2017**, *108*, 97–104. [CrossRef]
69. Brovko, O.; Palamarchuk, I.; Bogdanovich, N.; Ivakhnov, A.; Chukhchin, D.; Malkov, A.; Volkov, A.; Arkhilin, M.; Gorshkova, N. Structure and electrophysical properties of carbogels based on the interpolyelectrolyte complex lignosulfonate—Chitosan with various composition. *Micropor. Mesopor. Mat.* **2019**, *282*, 211–218. [CrossRef]
70. Izumrudov, V.A.; Mussabayeva, B.K.; Kassymova, Z.S.; Klivenko, A.N.; Orazzhanova, L.K. Interpolyelectrolyte complexes: Advances and prospects of application. *Russ. Chem. Rev.* **2019**, *88*, 1046–1062. [CrossRef]
71. Devaurs, D.; Antunes, D.A.; Hall-Swan, S.; Mitchell, N.; Moll, M.; Lizée, G.; Kavradi, L.E. Using parallelized incremental meta-docking can solve the conformational sampling issue when docking large ligands to proteins. *BMC Mol. Biol.* **2019**, *20*, 42. [CrossRef]

72. Antunes, D.A.; Moll, M.; Devaurs, D.; Jackson, K.R.; Lizée, G.; Kaviraki, L.E. DINC 2.0: A new protein-peptide docking webserver using an incremental approach. *Cancer Res.* **2017**, *77*, 55–57. [[CrossRef](#)]
73. Zhang, S.; Assaf, K.I.; Huang, C.; Hennig, A.; Nau, W.M. Ratiometric DNA sensing with a host-guest FRET pair. *Chem. Commun.* **2019**, *55*, 671–674. [[CrossRef](#)]
74. Rana, R.; Chang, Q.; Bassan, J.; Chow, S.; Hedley, D.; Nitz, M. An iodinated DAPI-based reagent for mass cytometry. *ChemBioChem* **2021**, *22*, 532–538. [[CrossRef](#)] [[PubMed](#)]
75. Deranleau, D.A. Theory of the measurement of weak molecular complexes. I. General considerations. *J. Am. Chem. Soc.* **1969**, *91*, 4044–4049. [[CrossRef](#)]
76. Shurpik, D.N.; Yakimova, L.S.; Rizvanov, I.K.; Plemenkov, V.V.; Stoikov, I.I. Water-soluble Pillar[5]arenes: Synthesis and characterization of the inclusion complexes with *p*-toluenesulfonic acid. *Macroheterocycles* **2015**, *8*, 128–134. [[CrossRef](#)]
77. Ziatdinova, R.V.; Nazarova, A.A.; Yakimova, L.S.; Mostovaya, O.A.; Kalinin, V.I.; Osin, Y.N.; Stoikov, I.I. Polyelectrolyte nanoparticles based on functionalized silica and Pillar[5]arene derivatives for recognition of model proteins. *Russ. Chem. Bull.* **2019**, *68*, 2065–2074. [[CrossRef](#)]